UNCLASSIFIED

AD NUMBER
AD323074

CLASSIFICATION CHANGES
TO: **unclassified**
FROM: **confidential**

LIMITATION CHANGES
TO: Approved for public release, distribution unlimited
FROM: Distribution authorized to U.S. Gov't. agencies and their contractors; Administrative/Operational Use; MAY 1961. Other requests shall be referred to National Aeronautics and Space Administration, Washington, DC.

AUTHORITY
NASA TR SERVER WEBSITE; NASA TR SERVER WEBSITE

THIS PAGE IS UNCLASSIFIED

TECHNICAL MEMORANDUM

X-526

LONGITUDINAL AERODYNAMIC CHARACTERISTICS OF

FIVE HYPERSONIC MISSILE CONFIGURATIONS

AT MACH NUMBERS FROM 2.01 TO 6.01

By George C. Ashby, Jr.

Langley Research Center
Langley Field, Va.

XEROX

NATIONAL AERONAUTICS AND SPACE ADMINISTRATION

WASHINGTON   May 1961

CONFIDENTIAL

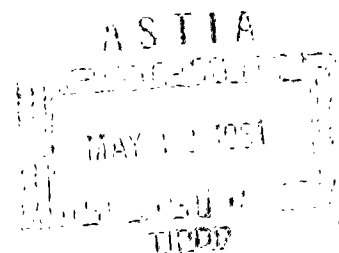NATIONAL AERONAUTICS AND SPACE ADMINISTRATION

TECHNICAL MEMORANDUM X-526

LONGITUDINAL AERODYNAMIC CHARACTERISTICS OF

FIVE HYPERSONIC MISSILE CONFIGURATIONS

AT MACH NUMBERS FROM 2.01 TO 6.01*

By George C. Ashby, Jr.

SUMMARY

Longitudinal aerodynamic characteristics of five hypersonic missile configurations have been determined in the Langley 20-inch hypersonic tunnel at a Mach number of 6.01 and a Reynolds number per foot of 6.96×10^6 for angles of attack up to $30°$. The configurations investigated were a body which had a length-diameter ratio of 10 and a cone-ogive nose, the body with a $10°$ flare, the body with cruciform fins of $5°$ or $15°$ apex angle, and a flared rocket model having a length-diameter ratio of 11.7 and a modified Von Kármán nose.

The results indicate that the configurations with the $10°$ flare or the $5°$ cruciform fins attain about the same normal-force and pitching-moment coefficients at $30°$ angle of attack but that the variation of pitching moment with angle of attack is more nearly linear for the flared model than for the model with $5°$ fins. Force and moment coefficients estimated by using Newtonian theory were found to be in good agreement with the measured values.

A summary of the data at Mach number 6.01 and previous data at Mach numbers from 2.01 to 4.65 indicates that with increasing Mach number, the slope of the normal-force curve decreases less for the flared bodies than for the finned bodies and the stability increases for the flared bodies, whereas it decreases for the finned bodies. A summary of data at several angles of attack indicates that the normal force and pitching moment (absolute) of the $5°$ cruciform finned model have a large rate of decrease with increasing Mach number in the range from Mach 2.01 to 3.75 and a low rate of decrease thereafter; whereas, for the flared model the rate of decrease of the normal force with Mach number is very low over the whole range and the absolute value of the pitching moment increases with Mach number.

---

*Title, Unclassified.

CONFIDENTIAL

TECHNICAL MEMORANDUM

X-526

LONGITUDINAL AERODYNAMIC CHARACTERISTICS OF

FIVE HYPERSONIC MISSILE CONFIGURATIONS

AT MACH NUMBERS FROM 2.01 TO 6.01

By George C. Ashby, Jr.

Langley Research Center
Langley Field, Va.

XEROX

NATIONAL AERONAUTICS AND SPACE ADMINISTRATION

WASHINGTON   May 1961

G

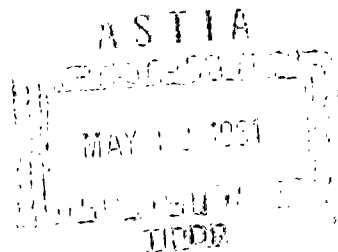NATIONAL AERONAUTICS AND SPACE ADMINISTRATION

TECHNICAL MEMORANDUM X-526

LONGITUDINAL AERODYNAMIC CHARACTERISTICS OF

FIVE HYPERSONIC MISSILE CONFIGURATIONS

AT MACH NUMBERS FROM 2.01 TO 6.01*

By George C. Ashby, Jr.

SUMMARY

Longitudinal aerodynamic characteristics of five hypersonic mis-
sile configurations have been determined in the Langley 20-inch hyper-
sonic tunnel at a Mach number of 6.01 and a Reynolds number per foot
of 6.96×10^6 for angles of attack up to $30°$. The configurations
investigated were a body which had a length-diameter ratio of 10 and
a cone-ogive nose, the body with a $10°$ flare, the body with cruciform
fins of $5°$ or $15°$ apex angle, and a flared rocket model having a length-
diameter ratio of 11.7 and a modified Von Kármán nose.

The results indicate that the configurations with the $10°$ flare or
the $5°$ cruciform fins attain about the same normal-force and pitching-
moment coefficients at $30°$ angle of attack but that the variation of
pitching moment with angle of attack is more nearly linear for the flared
model than for the model with $5°$ fins. Force and moment coefficients
estimated by using Newtonian theory were found to be in good agreement
with the measured values.

A summary of the data at Mach number 6.01 and previous data at
Mach numbers from 2.01 to 4.65 indicates that with increasing Mach number,
the slope of the normal-force curve decreases less for the flared bodies
than for the finned bodies and the stability increases for the flared
bodies, whereas it decreases for the finned bodies. A summary of data
at several angles of attack indicates that the normal force and pitching
moment (absolute) of the $5°$ cruciform finned model have a large rate of
decrease with increasing Mach number in the range from Mach 2.01 to 3.75
and a low rate of decrease thereafter; whereas, for the flared model the
rate of decrease of the normal force with Mach number is very low over
the whole range and the absolute value of the pitching moment increases
with Mach number.

*Title, Unclassified.

INTRODUCTION

Interceptor missiles to be used in defense against supersonic attack will probably be required to operate at hypersonic speeds. In this speed range the missile configuration design is influenced strongly by considerations of aerodynamic heating. Because of their comparatively low heating rates highly swept wings are being considered for use on hypersonic interceptor missiles. References 1 to 3 indicate that configurations of this type operating at supersonic speeds have a relatively low drag penalty if the leading edges are blunted to reduce aerodynamic-heating rates, have small induced rolling moments, small center-of-pressure shifts, high lift effectiveness (compared to wingless missiles), and are longitudinally and directionally stable. Reference 4 shows that blunting the leading edge of highly swept wings does not alter the normal-force coefficient very much at hypersonic speeds. Reference 5 indicates that wingless missiles with flared afterbodies may be satisfactory at supersonic speeds from stability considerations, although the lift capabilities are low and the drag penalty is high. In order to obtain more information on the aerodynamic characteristics of such configurations, an investigation of a series of missile configurations has been conducted by the National Aeronautics and Space Administration at supersonic and hypersonic speeds.

The models investigated include a basic body having an overall fineness ratio of 10 incorporating a cone-ogive nose and fitted in turn with a $10°$ flared afterbody and with two different sets of low-aspect-ratio cruciform fins. An additional model having an overall fineness ratio of 11.7, a $10°$ flared afterbody, and a modified Von Kármán nose was also tested. Models similar to the five used in the present investigation were previously tested in the Langley 4-foot supersonic pressure tunnel at a Mach number of 2.01 (ref. 5) and in the Langley Unitary Plan wind tunnel for the range of Mach numbers from 2.29 to 4.65 (ref. 6). In addition, the results of free-flight tests of the fineness-ratio-11.70 model with the flared afterbody are presented in reference 7 for Mach numbers up to 4.3 and the results of tests of the basic body with the $5°$ cruciform fins in the 26-inch Langley transonic blowdown and 9- by 12-inch blowdown tunnels at Mach numbers from 0.82 to 3.05 are presented in reference 8. The results of tests of the basic body with $5°$ cruciform fins and trailing-edge flaps and the basic body with a $10°$ flared afterbody equipped with all-movable controls are presented for Mach number 6.8 in reference 9 and for Mach numbers 2.01, 4.65, and 6.8 in reference 10.

The present paper contains the results of tests made in the Langley 20-inch Mach 6 tunnel to determine axial forces, normal forces, and pitching moments of the five models. The tests were made for angles of attack from $-4°$ to $30°$ at a Reynolds number based on body length of 10.44×10^6. Comparison of the measured coefficients with those

calculated by using Newtonian theory are also presented. In addition, the aerodynamic characteristics obtained for similar models at Mach number 2.01 and at Mach numbers 2.29 to 4.65 (refs. 5 and 6) are presented to show variation with Mach number.

SYMBOLS

The coefficients of forces and moments are referred to the body-axis system (fig. 1) and the pitching moment is taken about the 50-percent body station.

C_N normal-force coefficient, F_N/qA

C_A axial-force coefficient, F_A/qA (including base axial force)

C_A' axial-force coefficient, F_A'/qA (corrected for base axial force)

C_m pitching-moment coefficient, M_Y/qAd

x_{cp} distance from nose of body to center of pressure

F_N normal force (see fig. 1)

F_A axial force (see fig. 1)

F_A' corrected axial force

M_Y pitching moment (see fig. 1)

M Mach number

d diameter of cylindrical section of body

l length of body

q free-stream dynamic pressure

A cross-sectional area of cylindrical section of body

α angle of attack of body center line, deg

x station measured from nose tip, in.

r   radius of cross section at given body station

R   radius of curvature

APPARATUS AND METHODS

Tunnel

The tests were made in the Langley 20-inch Mach 6 tunnel which is
described in reference 11. The tunnel is of the blowdown to atmosphere
type capable of operation at a maximum pressure of 580 psi and a maxi-
mum temperature of 600° F.

Models

The geometric characteristics of the models are given in table I
and figure 2. A photograph of the five models is presented as figure 3.
Models I to IV (fig. 2) employed the same basic body, which had a nominal
fineness ratio of 10. The forebody contour for these models consisted of
a combination straight section and a circular arc. Model I was the basic
configuration with a cylindrical afterbody. Models II to IV utilized
this same basic body but, in addition, incorporated either a 10° flare or
cruciform fins with 5° or 10° "apex" angles. (The fin apex angle is actu-
ally the complement of the leading-edge sweep.) Model V (fig. 2) was
similar to the fineness-ratio-11.7 model with a 10° flare investigated in
references 5 to 7. This model had a Von Kármán forebody with a rounded
nose.

The models were supported in the tunnel by the "gooseneck" support
shown in figure 4. A photograph of model III mounted in the tunnel is
shown in figure 5. With the support mounted from the top as shown in
figures 4 and 5, the horizontal plane is the angle-of-attack plane. An
optical system described in reference 11 was used to set angle of attack.

Normal force, axial force, and pitching moment were measured by means
of a water-cooled, internally mounted, strain-gage balance.

Test Conditions and Accuracy

Tests.- All tests were made at a stagnation temperature of 400° F,
a stagnation pressure of 365 lb/sq in. absolute, and a Mach number of 6.01.
The Reynolds number per foot was 6.96×10^6. Tests were made through an
angle-of-attack range from -4° to 30° at zero sideslip.

Accuracy.- The calibrated Mach number variation in the region of the test model was no more than ±0.01. The values of angle of attack are estimated to be accurate to within ±0.1°. The maximum errors in the coefficients from these tests based on inherent balance error, zero shifts, and pressure variation are as follows:

C_N . . . . ±0.155
C_A . . . . ±0.044
C_m . . . . ±0.138

RESULTS AND DISCUSSION

Aerodynamic Characteristics in Pitch at M = 6.01

The pitching-moment, axial-force, and normal-force coefficients and the center-of-pressure location in percent body length are plotted against angle of attack in figures 6 to 10 for the five models at a Mach number of 6.01 and are presented in summary form in figures 11 and 12. It should be noted that the axial force has not been corrected for base-pressure effect. Because of the differences in the planforms and total planform areas, the coefficients are based on the cross-sectional area of the cylindrical section of the basic body, and the results are discussed in terms of the effects of adding a flare or fins to the basic body.

The results of figures 11 and 12 indicate that adding a flare or cruciform fins to the basic body results in an appreciable increase in normal force, in the absolute magnitude of pitching moment, and in axial force, and a reduction in the variation of the center-of-pressure location with angle of attack. The addition of the flare (fig. 7) and the addition of the 5° fins (fig. 8) increases the normal force approximately the same amount and attains about the same restoring moment at the highest angles of attack. However, the flare improves the stability (more negative slope of pitching-moment curve) a greater amount than the fins in the lower angle-of-attack range. Of course, the axial-force increase is very much larger for the flare than for the 5° fins. The addition of the 15° fins (fig. 12) is not as effective in producing pitching moment and normal force as the addition of the 5° fin because of the area and fin-body interference differences; in addition, the axial-force increase is larger for the 15° fin because of higher leading-edge axial force.

It is interesting to note that the longer body and shorter flare (model V) achieved approximately the same normal force and pitching moment with a smaller increase in axial force than the basic body with the flare (model II). (See fig. 11.)

The estimated aerodynamic characteristics shown in figures 6 to 9 were computed by using the unmodified Newtonian theory. For the basic body (fig. 6) the coefficients were determined by the method of reference 12. For the finned and flared models the values for the forebody and afterbody sections were calculated separately and added. Contributions of the forebody and the flare were obtained from reference 12, and the shielding effects of the forebody on the flare or fins were ignored. For the finned portion of the configurations the projected area of the body as well as the fins was treated as a flat plate and C_N was determined by using $2 \sin^2\alpha$. In these finned models the contribution of the leading edges of the four fins was included.

The estimated normal-force coefficient and the center-of-pressure location in general are in good agreement with the measured values. The effect of ignoring the shielding effects for the body with flare can be seen at the higher angles of attack in figure 7. The measured values of normal force and pitching moment are higher than those estimated because the shielding eliminates a portion of the surface which produces a negative normal force and a forward movement of the center of pressure. The effect of ignoring the shielding for the finned bodies (figs. 8 and 9) would not be large since the contribution of the upper fin is small. The agreement between the estimated and measured pitching-moment coefficient is good considering that the accuracy of the estimated value is affected strongly by the accuracy of the estimated normal-force coefficient - the inaccuracy in the estimated pitching moment being due to the inaccuracy of the estimated center of pressure (which in this case is considered quite small) and the inaccuracy in the estimated normal-force coefficient. This effect is large in the case of the flared body at the higher angles of attack (fig. 7). The axial-force coefficients estimated by the unmodified Newtonian theory follow the trend of the measured values with angle of attack; however, the values are not directly comparable to the measured values because they do not include skin friction or base-pressure effects.

Since no base-pressure measurements were made, the estimated axial-force coefficients at each angle of attack were adjusted by approximating a constant base-pressure coefficient equal to $-1/M^2$ and subtracting it from the Newtonian values. For the basic body and the finned body the free-stream Mach number was used but for the flared body the Mach number was taken as that behind the oblique shock on a wedge having the same angle as the flare immersed in a Mach 6.01 flow. It was felt that this Mach number was more applicable because of the effects of the flare shock. The base-pressure coefficients of both the flared and finned bodies were adjusted for the increased base area. The agreement between the estimated and measured axial-force coefficients of the basic body and flared body are shown to be very good in figures 6 and 7. The agreement for the finned bodies is not so good (figs. 8 and 9) because no correction for fin effect on the base pressure was made. Reference 13 shows that at lower Mach

numbers the addition of fins to a body of revolution decreases the
base-pressure coefficient (increases negatively).

Variation of Aerodynamic Characteristics in Pitch With Mach Number

Figure 13 presents the pitching-moment, axial-force, and normal-
force coefficients, and the center-of-pressure location in percent body
length as a function of angle of attack for the five models at Mach
numbers 2.01, 3.22, 4.65, and 6.01. The data at Mach number 2.01 were
obtained from reference 5 and that at Mach numbers 3.22 and 4.65 were
obtained from reference 6.

The slope of the curve of normal-force coefficient against angle
of attack decreases with increasing Mach number for all five bodies;
however, the decrease for the basic body and the flared bodies is small
compared with that of the finned bodies. The stability (slope of the
pitching-moment curve) decreases with Mach number for the finned bodies
but increases for the others. The random change of the variation of the
center-of-pressure location with angle of attack as Mach number increases
is a magnification of the small errors in normal force and pitching moment
especially at the low angle of attack; however, in general the center of
pressure moves rearward on the basic and flared bodies but moves forward
on the finned bodies as Mach number increases. The variation of the axial-
force coefficient with increasing angle of attack tends to change from an
undulating type of variation to a continuously increasing type of variation
as Mach number increases from 2.01 to 6.01.

In order to show the effect of Mach number on the coefficient at a
fixed angle of attack, the data at angles of attack of 8°, 16°, and 24°
are plotted against Mach number in figure 14. In general the normal-
force coefficient of each configuration decreases with increasing Mach
number at all three angles of attack. However, the rate of change for
the flared models II and V is very slight. Above a Mach number 3.75 the
rate of change of normal force with Mach number is quasi-linear and nearly
equal for the basic body and the two finned models. Below this Mach number
the basic body (model I) and the body with 15° fins (model IV) retain this
relationship but the body with 5° fins (model III) has a much larger rate
of change.

At all three angles of attack the absolute magnitude of the pitching-
moment coefficient decreases as Mach number increases for the finned models
but increases for the flared models. For the flared models the normal-
force coefficient decreases only slightly with increasing Mach number and
the center of pressure moves rearward; whereas, for the finned models the
decrease in normal force is larger and the center of pressure moves for-
ward. In the case of the center-of-pressure curves at $\alpha = 8°$

(fig. 14(a)), it should be mentioned that the fairings were made by using the curves at $\alpha = 16°$ and $24°$ as a guide, because the smaller values of normal-force and pitching-moment coefficients at $\alpha = 8°$ results in considerably more scatter than at the other angles of attack.

A base block was used in the tests of reference 6 to make the base pressure uniform across the base. Therefore, in order to compare the axial-force coefficients of those tests with the values of the present investigation, the axial-force coefficients were adjusted for base-pressure effects (identified by the prime). The base axial-force coefficients given in figure 5 of reference 6 were subtracted from the measured axial-force coefficients reported therein. The base-pressure coefficient of the present investigation was assumed to be equal to $-1/M^2$ and the axial-force coefficients were corrected to a value corresponding to free-stream static pressure on the base. The axial-force coefficients for the long flared body, model V, are not included in figure 14 because no base-pressure-coefficient corrections were available in reference 6. The results of figure 14 show that the axial-force coefficients of the four models have the same trend with Mach number. At $\alpha = 8°$ the axial-force coefficient decreases with Mach number but at $\alpha = 16°$ and $24°$ the coefficients increase with Mach number. The variation with Mach number is greatest for the flared body.

L
9
3
4

CONCLUSIONS

An experimental investigation of several hypersonic missile configurations has been conducted at Mach number 6.01. The configurations included a basic fineness-ratio-10 body and the same body with a 10° flare or with 5° or 15° cruciform fins. In addition, a fineness-ratio-11.7 flared model with a modified Von Kármán nose was tested. The data obtained at Mach number 6.01 are compared with predictions based on Newtonian theory. In addition the Mach 6.01 data are presented with data from previous investigations at lower Mach numbers. The results indicate the following conclusions:

1. At Mach number 6.01 the addition of flared skirts or cruciform fins to the basic body results in an appreciable increase in the normal-force, the absolute magnitude of the pitching-moment, and the axial-force coefficients and a reduction in the movement of the center-of-pressure location with angle of attack.

2. At Mach number 6.01 the addition of the flared skirt or the 5° cruciform fins to the basic body resulted in approximately the same normal-force and pitching-moment increase at the higher angles of attack but the flared skirt improved the stability more at the low angles of

attack. The increase of axial force is greater with the addition of the flared skirt than with the addition of the fins.

3. The normal-force and pitching-moment coefficients and the center-of-pressure location for hypersonic missile configurations can be determined with reasonable accuracy by using the Newtonian theory. The estimated axial-force coefficient consisting of the sum of the Newtonian value plus an approximation of the base-pressure coefficient was in good agreement with the measured values for the basic and flared bodies but underestimated the experimental values for the finned bodies.

4. The slope of the normal-force-coefficient curve of the finned bodies decreases more with increasing Mach number than that of the basic and flared bodies. The stability (slope of the pitching-moment curve) decreases with increasing Mach number for the finned bodies but increases for the basic and flared bodies. The axial-force coefficient at a Mach number of 2.01 undulates with increasing angle of attack especially for the flared bodies but changes to a continuously increasing variation with angle of attack as Mach number increases.

5. The normal-force coefficient and the absolute value of the pitching-moment coefficient of the 5° cruciform finned model have a large rate of decrease with increasing Mach number in the Mach number range from 2.01 to 3.75 and a low rate of decrease at higher Mach numbers; whereas, for the flared model, the rate of decrease of the normal-force coefficient with Mach number is very low over the whole range and the absolute magnitude of the pitching-moment coefficient increases with Mach number. Axial-force coefficients of all the models decrease as Mach number increases at low angles of attack but the trend reverses at the higher angles of attack.

Langley Research Center,
    National Aeronautics and Space Administration,
        Langley Field, Va., February 14, 1961.

REFERENCES

1. Robinson, Ross B.: Aerodynamic Characteristics of Missile Configuration With Wings of Low Aspect Ratio for Various Combinations of Forebodies, Afterbodies, and Nose Shapes for Combined Angles of Attack and Sideslip at a Mach Number of 2.01. NACA RM L57D19, 1957.

2. Katzen, Elliott D., and Jorgensen, Leland H.: Aerodynamics of Missiles Employing Wings of Very Low Aspect Ratio. NACA RM A55L13b, 1956.

3. Jorgensen, Leland H., and Katzen, Elliott D.: Wing-Body Combinations With Wings of Very Low Aspect Ratio at Supersonic Speeds. NACA RM A56G16, 1956.

4. Nicholson, Kenneth F.: The Effect of Blunt Leading Edges on Delta Wings at Mach 5.8. Jour. Aero/Space Sci. (Readers' Forum), vol. 25, no. 12, Dec. 1958, pp. 786-787.

5. Robinson, Ross B.: Wind-Tunnel Investigation at a Mach Number of 2.01 of the Aerodynamic Characteristics in Combined Angles of Attack and Sideslip of Several Hypersonic Missile Configurations With Various Canard Controls. NACA RM L58A21, 1958.

6. Turner, Kenneth L., and Appich, W. H., Jr.: Investigation of the Static Stability Characteristics of Five Hypersonic Missile Configurations at Mach Numbers From 2.29 to 4.65. NACA RM L58D04, 1958.

7. Bland, William M., Jr., and Kolenkiewicz, Ronald: Free-Flight Pressure Measurements Over a Flare-Stabilized Rocket Model With a Modified Von Kármán Nose for Mach Numbers Up to 4.3. NACA RM L57J24, 1958.

8. Swihart, John M.: An Investigation of the Static Stability and Control Characteristics of Winged and Wingless Interceptor Missile Models. NASA TM X-202, 1959.

9. Robinson, Ross B., and Bernot, Peter T.: Aerodynamic Characteristics at a Mach Number of 6.8 of Two Hypersonic Missile Configurations, One With Low-Aspect-Ratio Cruciform Fins and Trailing-Edge Flaps and One With a Flared Afterbody and All-Movable Controls. NACA RM L58D24, 1958.

L
9
3
4

L
9
3
4

10. Spearman, M. Leroy, and Robinson, Ross B.: Longitudinal Stability and Control Characteristics at Mach Numbers of 2.01, 4.65, and 6.8 of Two Hypersonic Missile Configurations, One Having Low-Aspect-Ratio Cruciform Wings With Trailing-Edge Flaps and One Having a Flared Afterbody and All-Movable Controls. NASA TM X-46, 1959.

11. Ashby, George C., Jr., and Fitzgerald, Paul E., Jr.: Longitudinal Stability and Control Characteristics of a Missile Configuration Having Several Highly Swept Cruciform Fins and a Number of Trailing Edge and Fin-Tip Controls at Mach Numbers From 2.21 to 6.01. NASA TM X-335, 1961.

12. Rainey, Robert W.: Working Charts for Rapid Prediction of Force and Pressure Coefficients on Arbitrary Bodies of Revolution by Use of Newtonian Concepts. NASA TN D-176, 1959.

13. Love, Eugene S.: Base Pressure at Supersonic Speeds on Two-Dimensional Airfoils and on Bodies of Revolution With and Without Fins Having Turbulent Boundary Layers. NACA TN 3819, 1957. (Supersedes NACA RM L53C02.)

CONFIDENTIAL

TABLE I.- MODEL DIMENSIONS

	Model I	Model II	Model III	Model IV	Model V
Body:					
Length, in.	18.040	17.972	17.986	17.970	21.064
Diameter, in.	1.798	1.798	1.800	1.800	1.798
Cross-sectional area, sq in.	2.539	2.539	2.545	2.545	2.539
Fineness ratio of nose	5.000	5.000	5.000	5.000	5.000
Fineness ratio of body	10.033	9.995	9.992	9.983	11.715
Moment center location, percent length	50.000	50.000	50.000	50.000	50.000
Flare:					
Length, in.		3.600			2.788
Base diameter, in.		3.068			2.782
Base area, sq in.		7.393			6.079
Flare angle, deg		10.000			10.000
Fins:					
Area exposed, 2 fins, sq in.			10.830	3.379	
Root chord, in.			11.460	3.508	
Tip chord, in.			0	0	
Span exposed, in.			1.920	1.926	
Span total, in.			3.720	3.726	
Taper ratio			0	0	
Aspect ratio exposed			0.340	1.098	
Span-diameter ratio			2.066	2.070	
Complement of sweepback angle, deg			5	15.35	

L-934
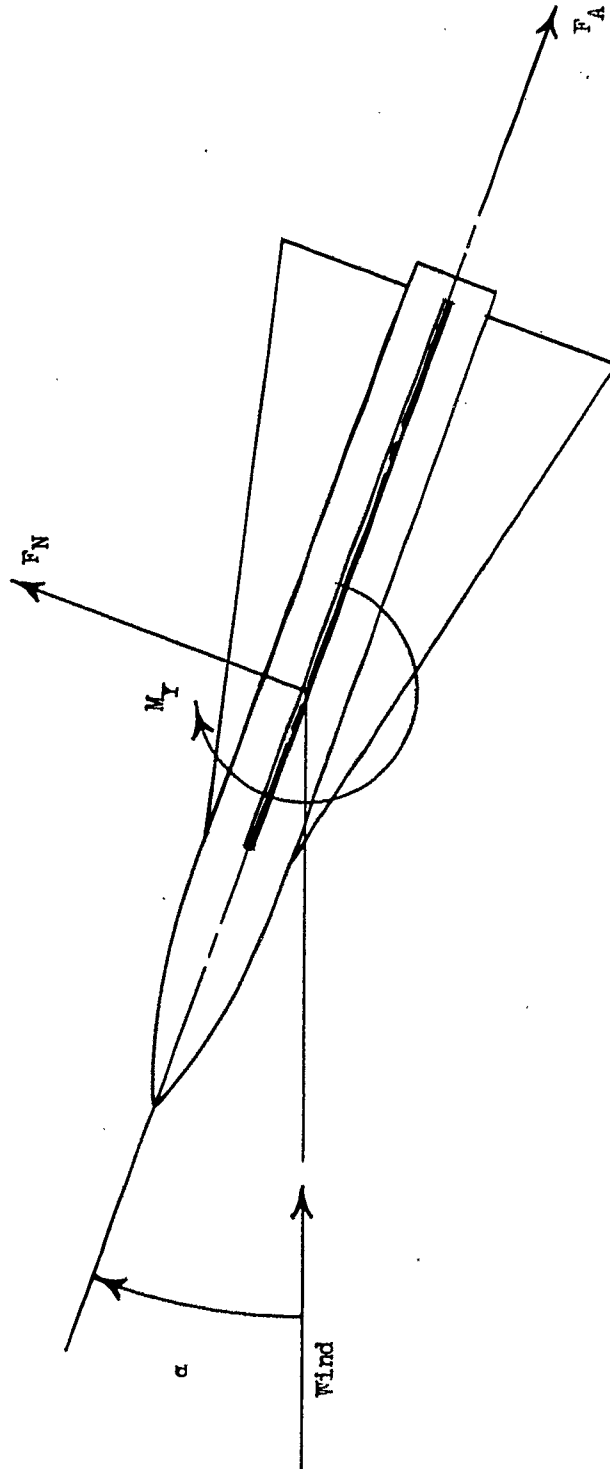
CONFIDENTIAL

L-934

Figure 1.- Body-axis system. Arrows indicate positive direction of forces, moments, and angles.

Coordinates of nose of models I, II, III, and IV	
x, in.	r, in.
0	---
0.18	0.18
3.60	.578
4.20	.644
4.80	.706
5.40	.758
6.0	.801
6.6	.837
7.2	.864
7.8	.884
8.4	.896
9.0	.900

Coordinates of nose of model V	
x, in.	r, in.
0	0
.032	.032
.855	.180
1.004	.205
1.305	.254
1.604	.297
1.904	.338
2.052	.360
2.203	.378
2.504	.416
2.804	.452
2.882	.461
3.703	.551
4.603	.635
5.503	.713
6.408	.778
7.290	.833
8.203	.877
9.103	.900

Model I, basic body

Model II, body with 10° flare

Model III, body with 5° fins

Model IV, body with 15° fins

Model V, hypersonic test vehicle

Figure 2.- Details of models.   Linear dimensions are in inches.

L-934
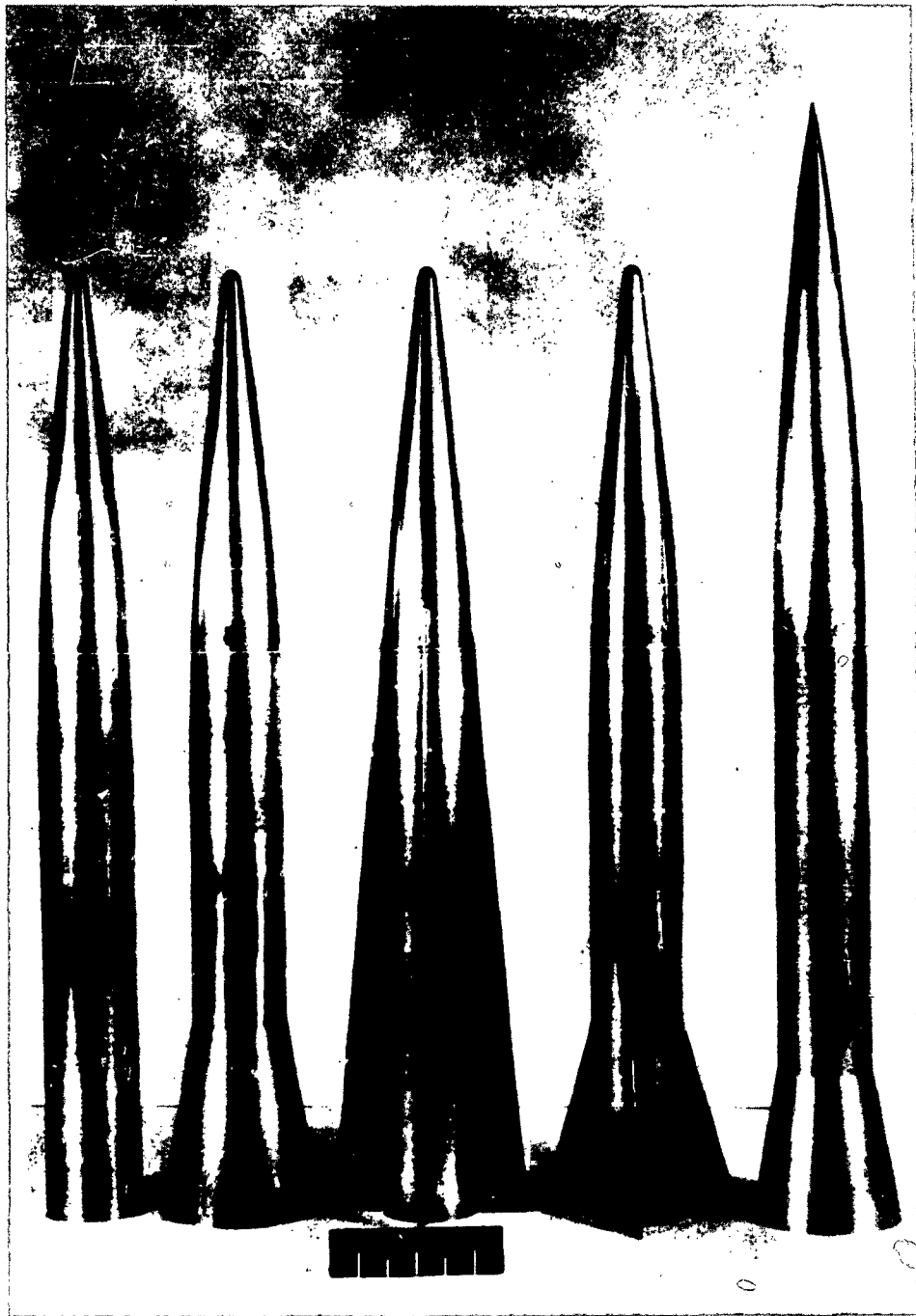
L-934

Figure 3.- Photograph of the five models.   L-60-746
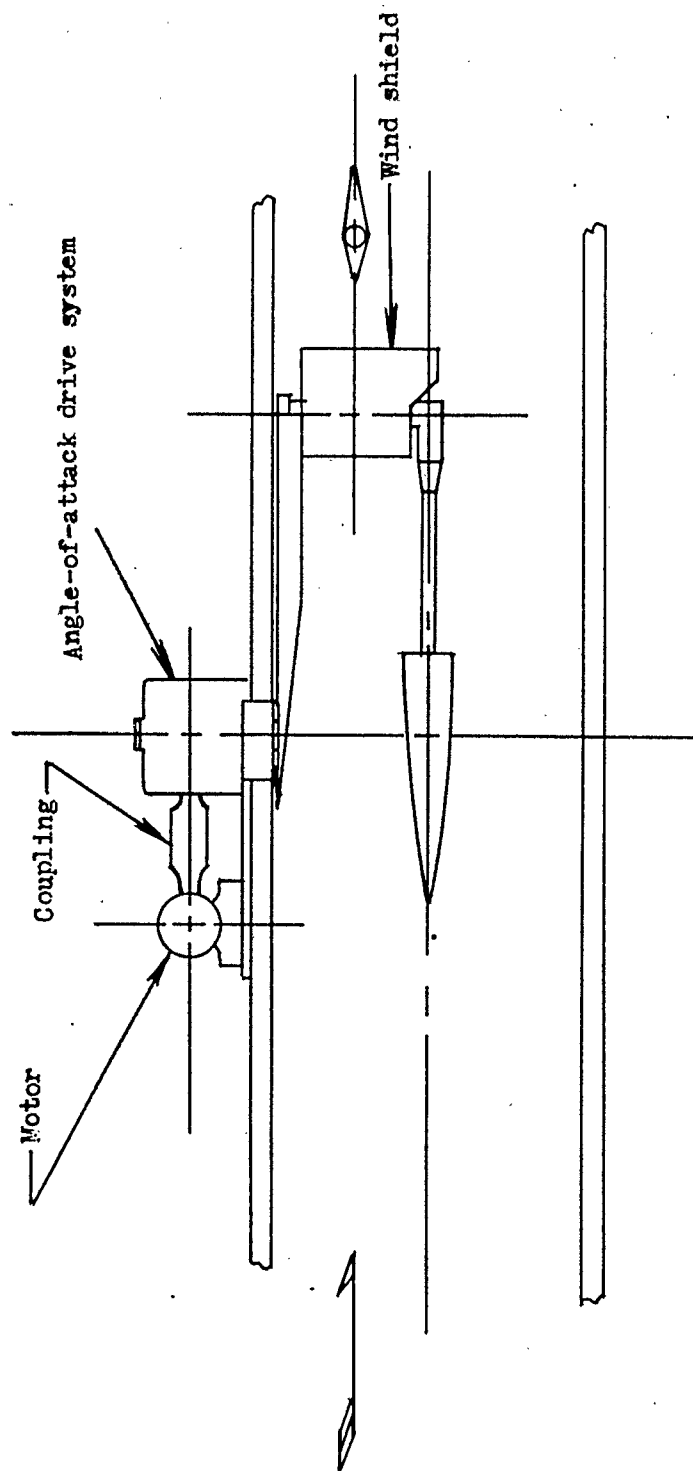
L-934

Figure 4.- Schematic diagram of the model-support system.

Figure 5.- Model III with 5° fins mounted in tunnel.

L-60-747

L-934
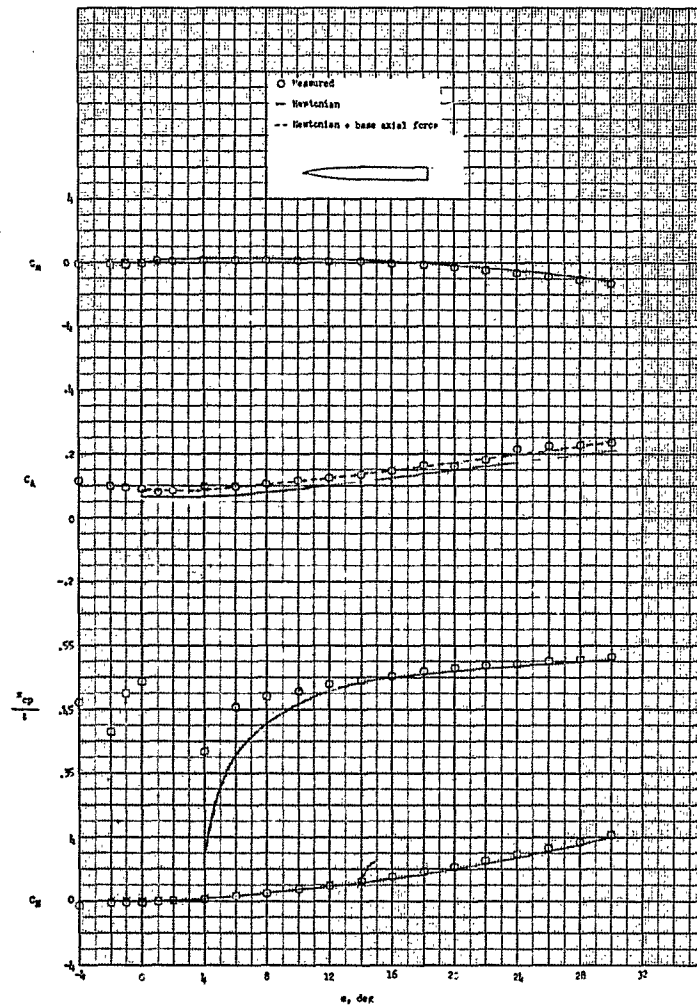
CONFIDENTIAL

Figure 6.- Aerodynamic characteristics of model I in pitch at M = 6.01.
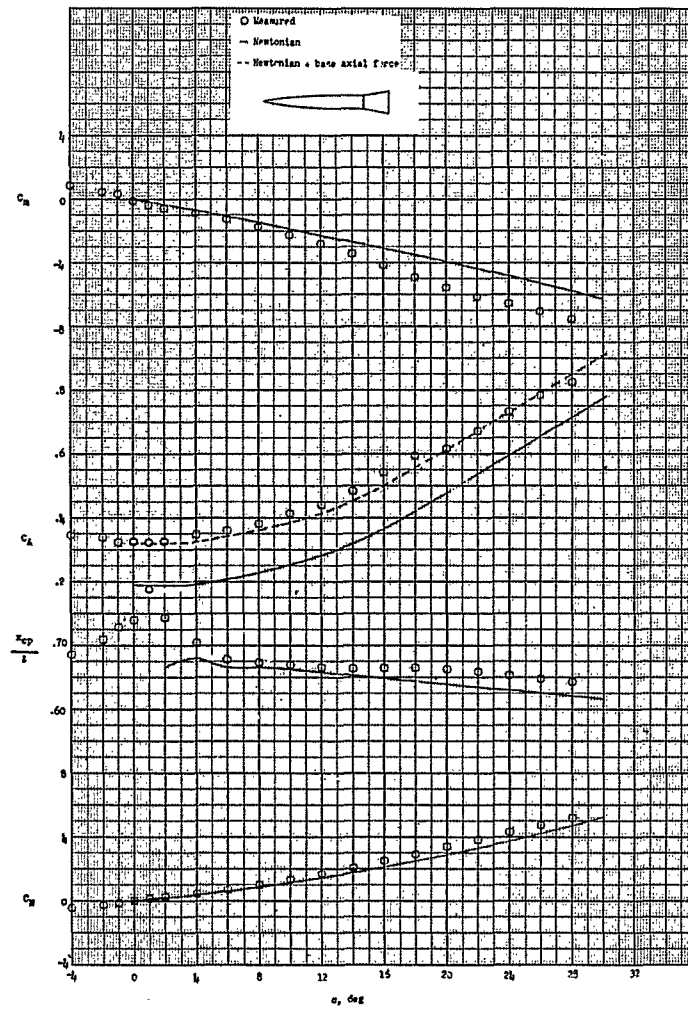
CONFIDENTIAL

Figure 7.- Aerodynamic characteristics of model II in pitch at M = 6.01.
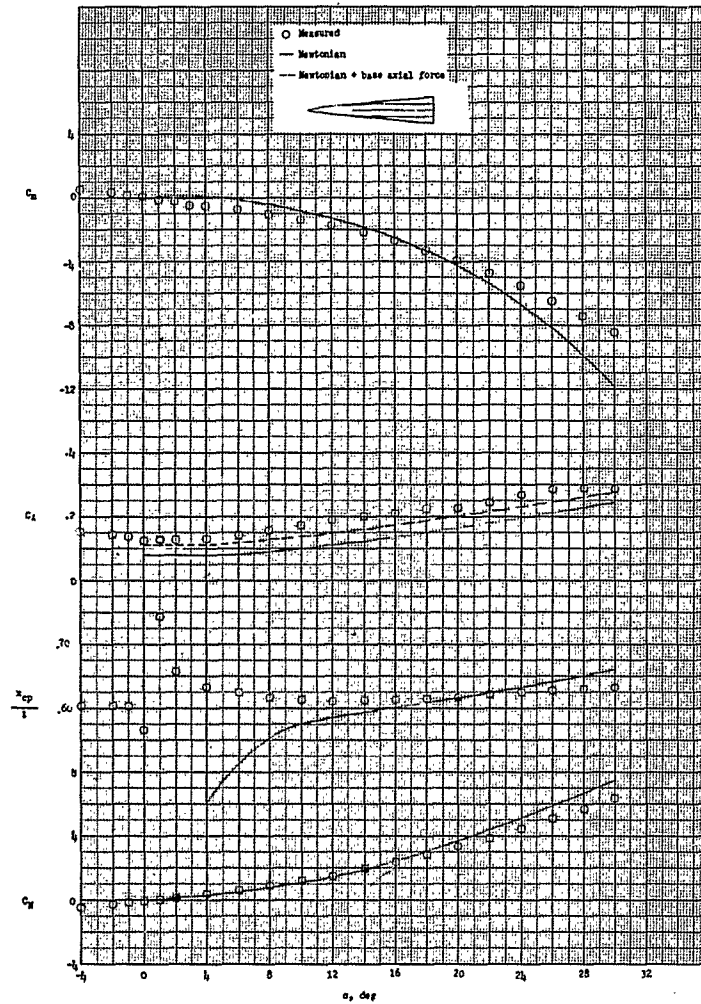
Figure 8.- Aerodynamic characteristics of model III in pitch at
M = 6.01.
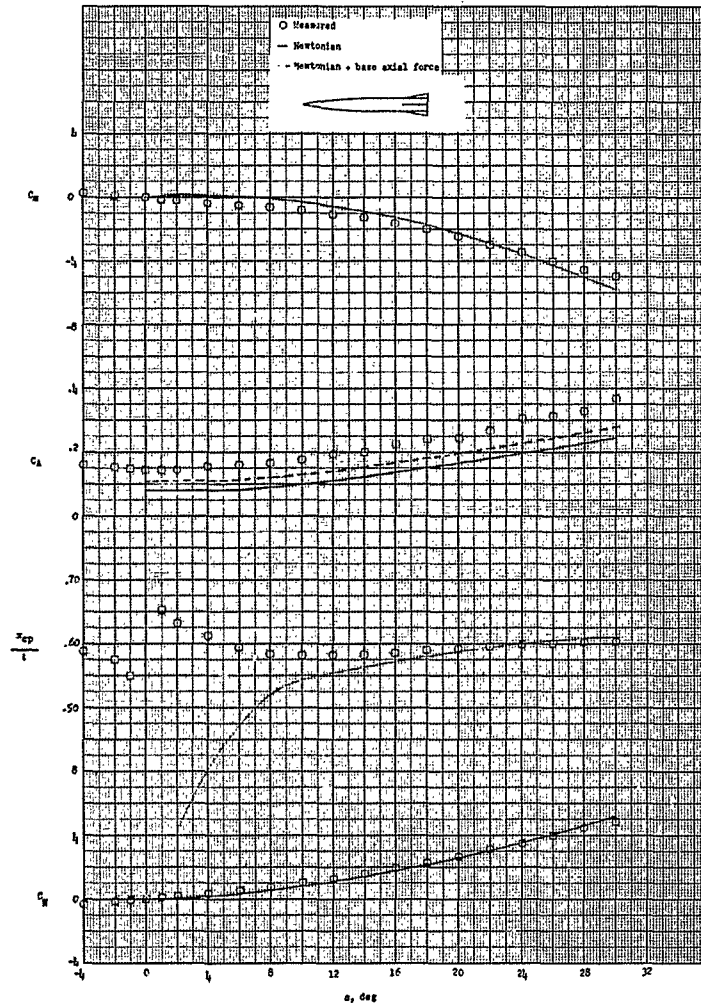
L-934

Figure 9.- Aerodynamic characteristics of model IV in pitch at M = 6.01.
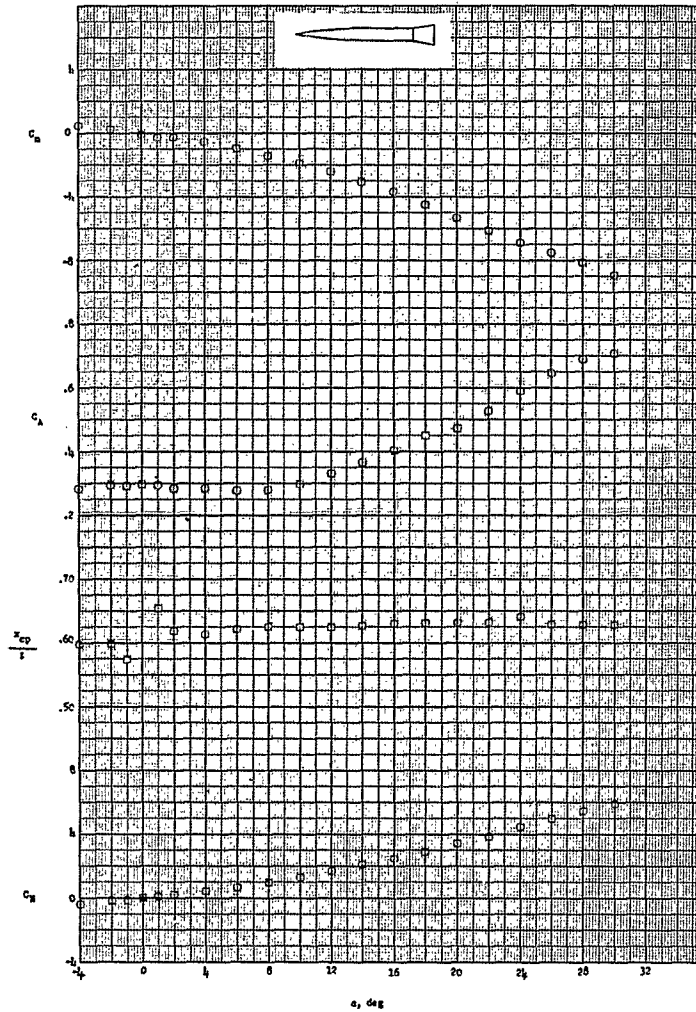
Figure 10.- Aerodynamic characteristics of model V in pitch at M = 6.01.
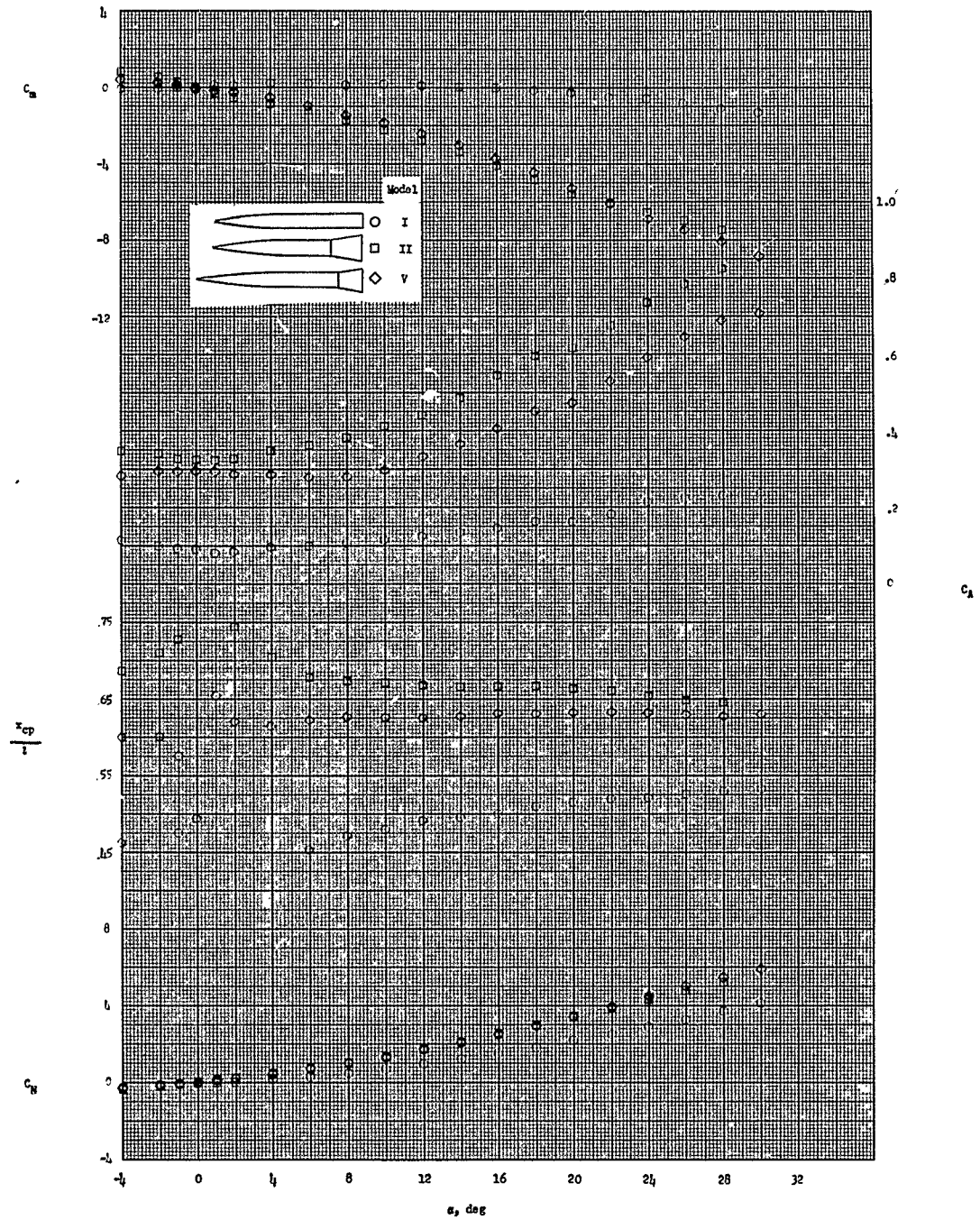
Figure 11.- Effects of afterbody flare on the aerodynamic characteristics in pitch at M = 6.01.
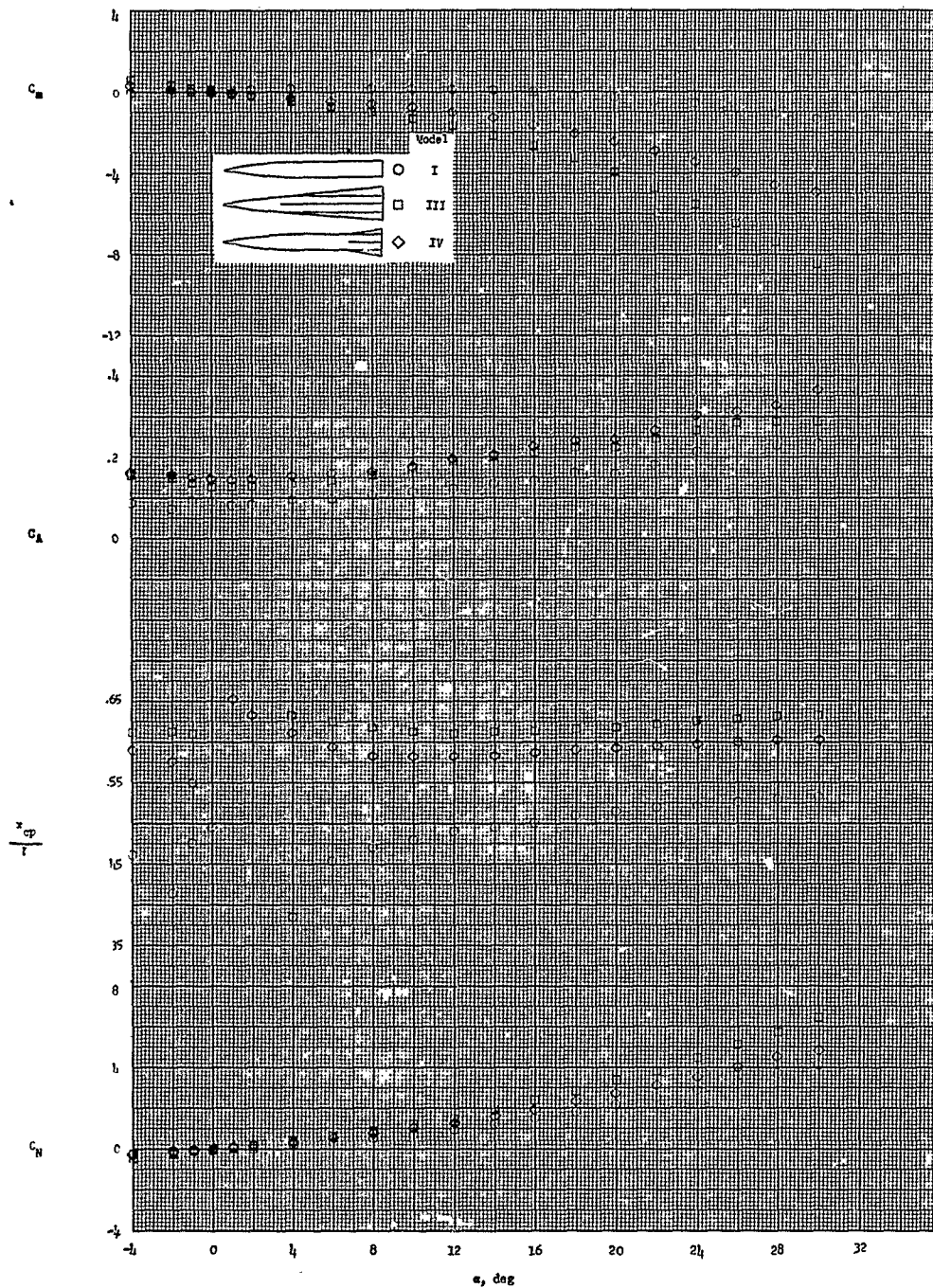
Figure 12.- Effects of fin planform on the aerodynamic characteristics in pitch at M = 6.01.

L-934

(a) Model I.

Figure 13.- Aerodynamic characteristics of the five models in pitch for
Mach numbers 2.01 to 6.01.
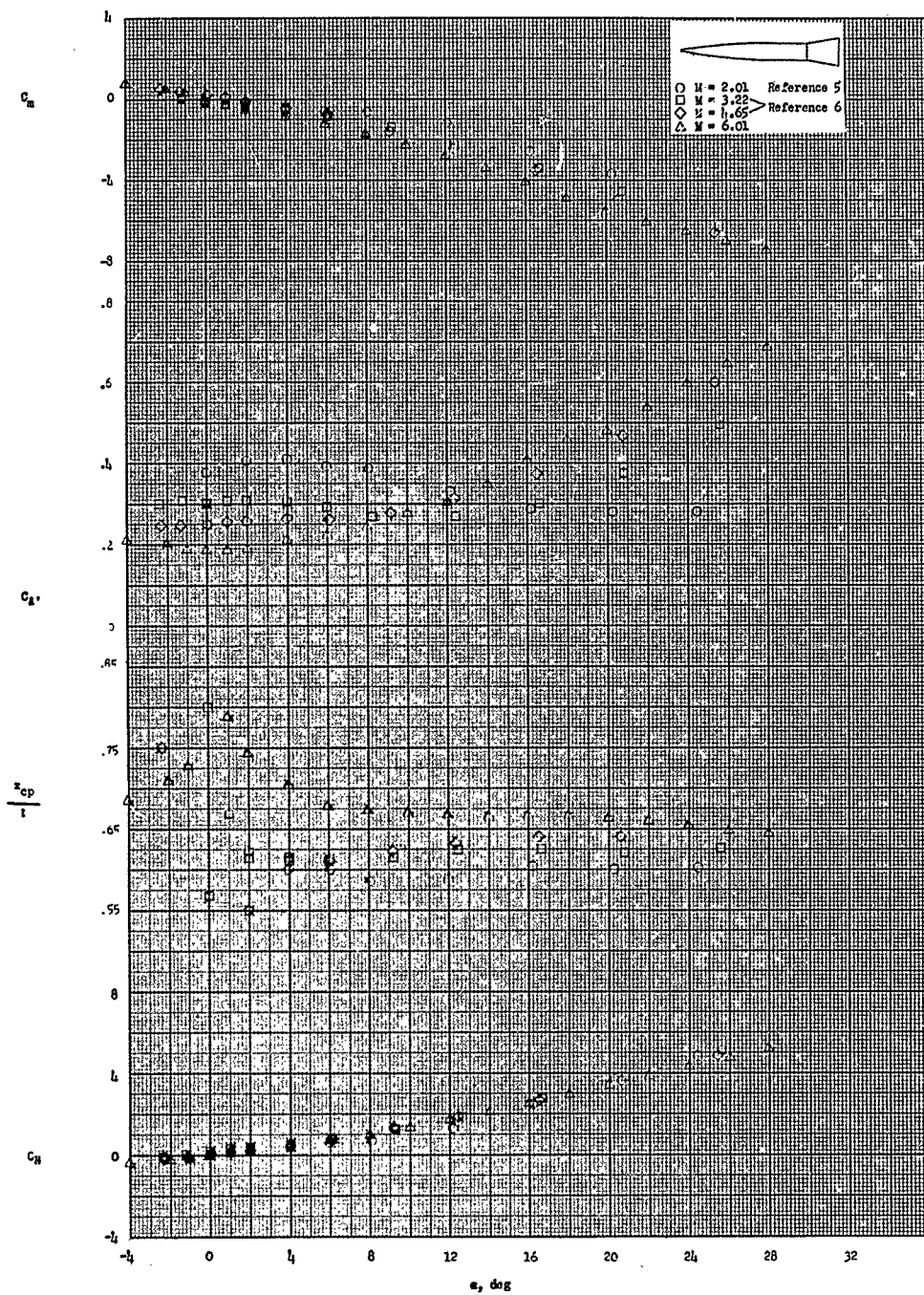
(b) Model II.

Figure 13.- Continued.

CONFIDENTIAL
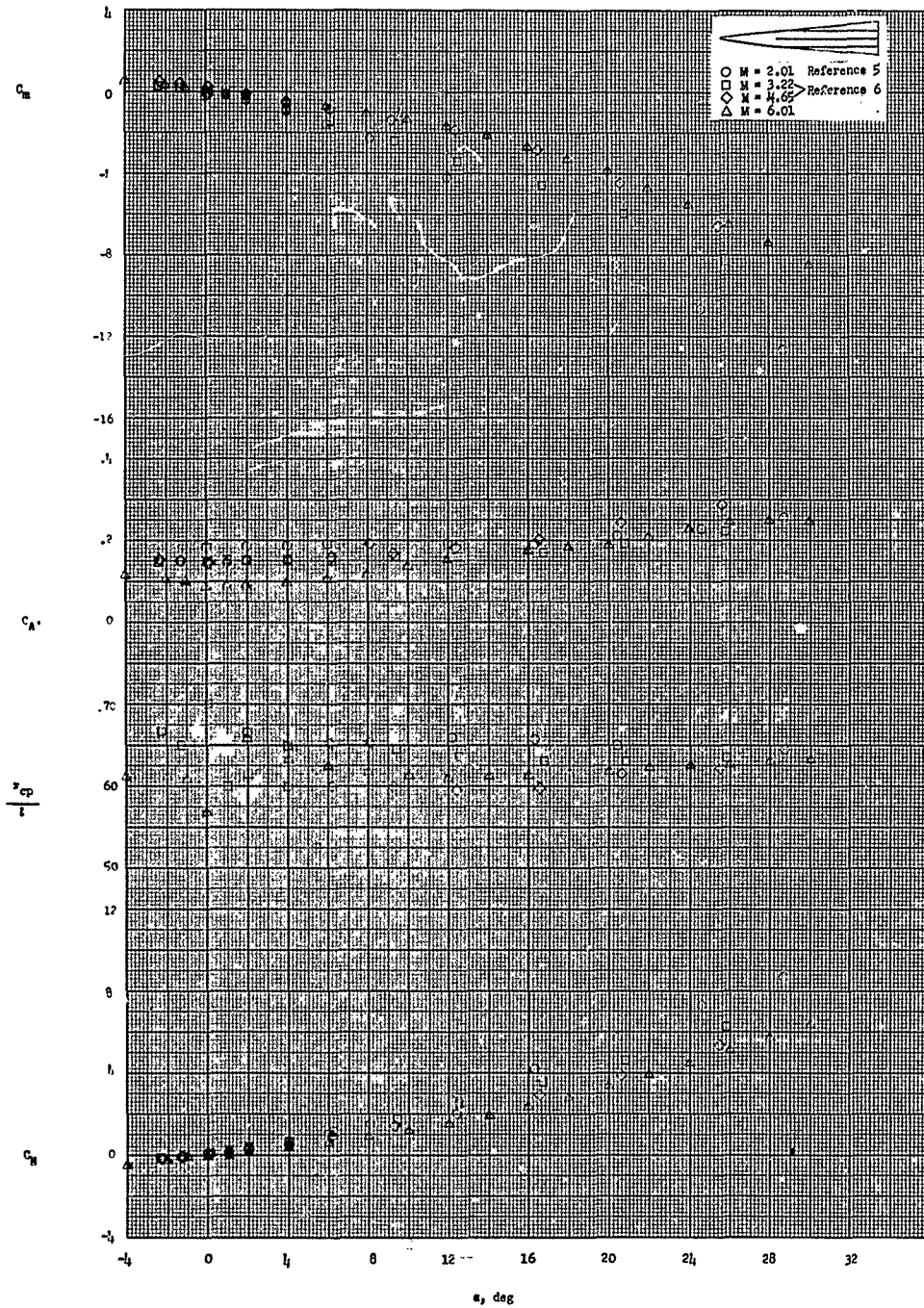
(c) Model III.

Figure 13.- Continued.
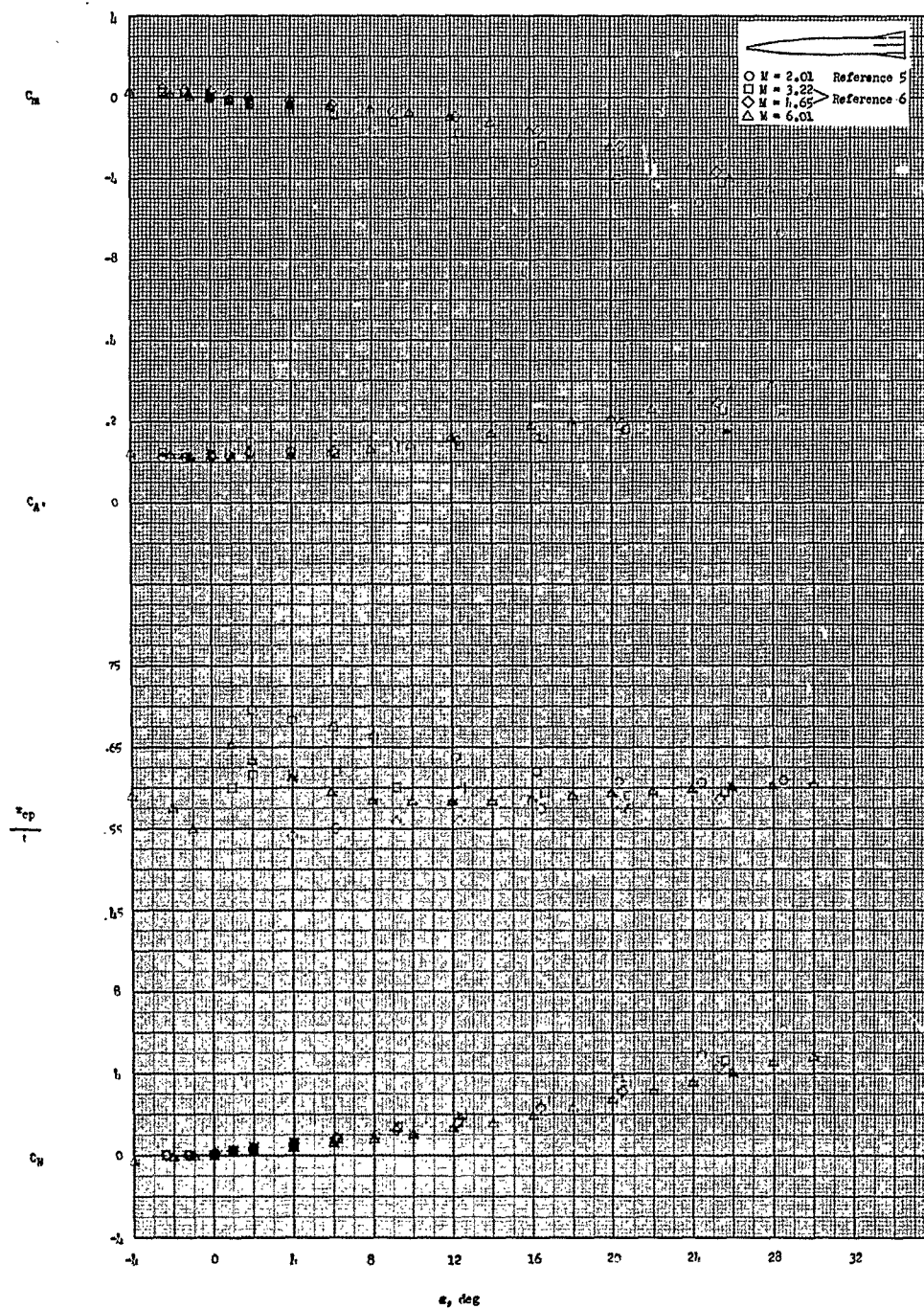
L-934

(d) Model IV.

Figure 13.- Continued.
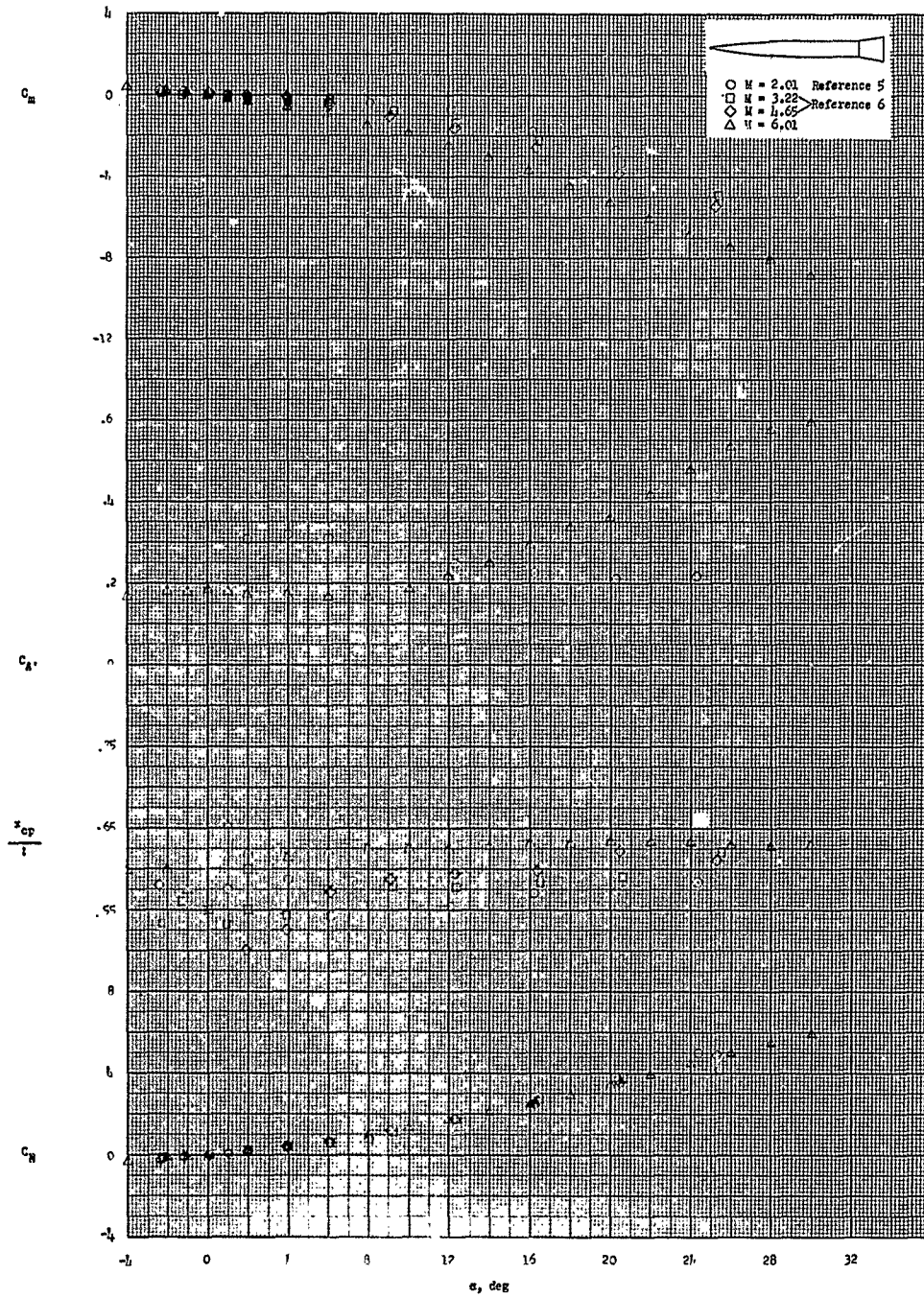
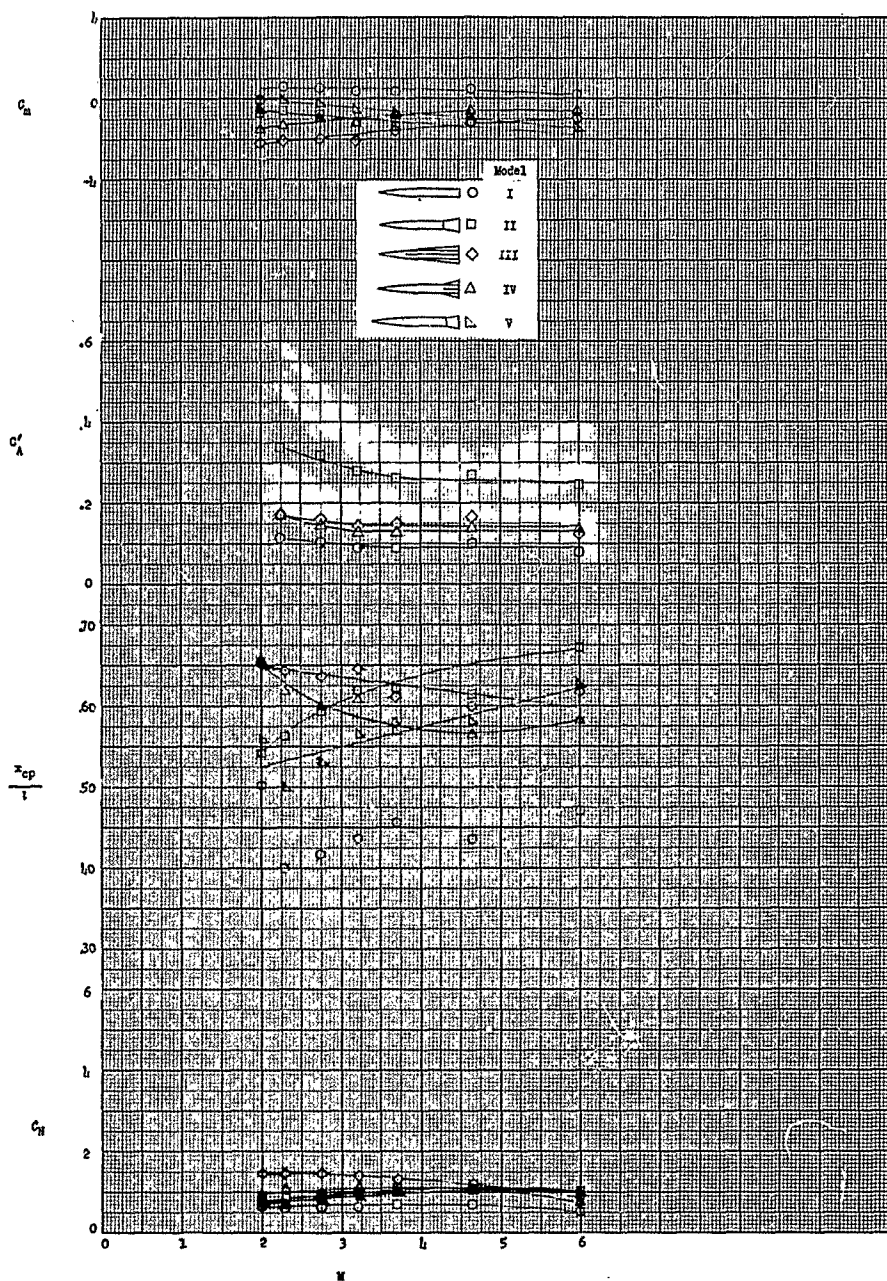L-934

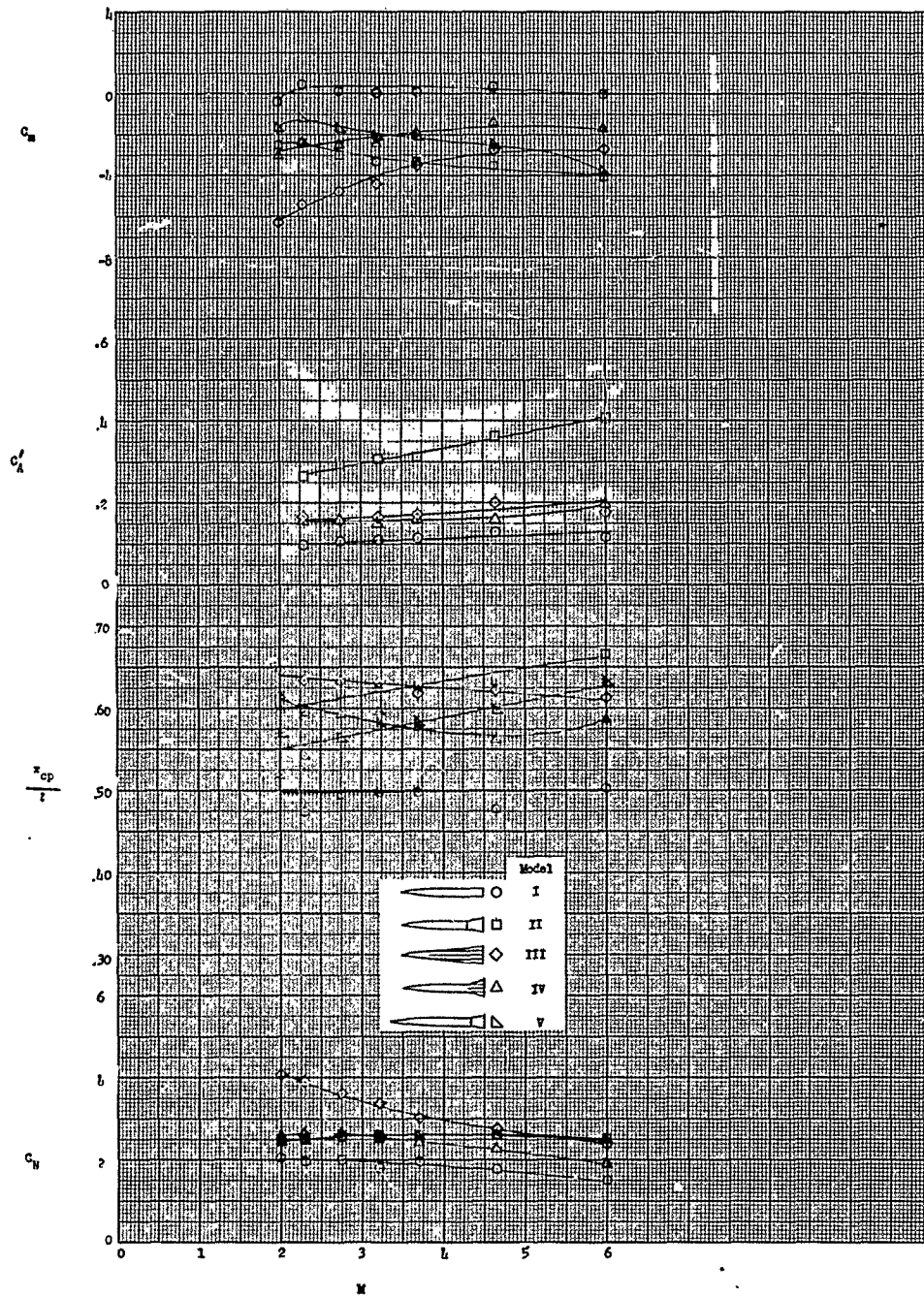
(e) Model V.

Figure 13.- Concluded.

CONFIDENTIAL

(a) $\alpha = 8^{\circ}$.

Figure 14.- Variation of the aerodynamic characteristics of the five
models with Mach number.   Data at   M = 2.01   and at 2.29 through
4.65 from references 5 and 6, respectively.
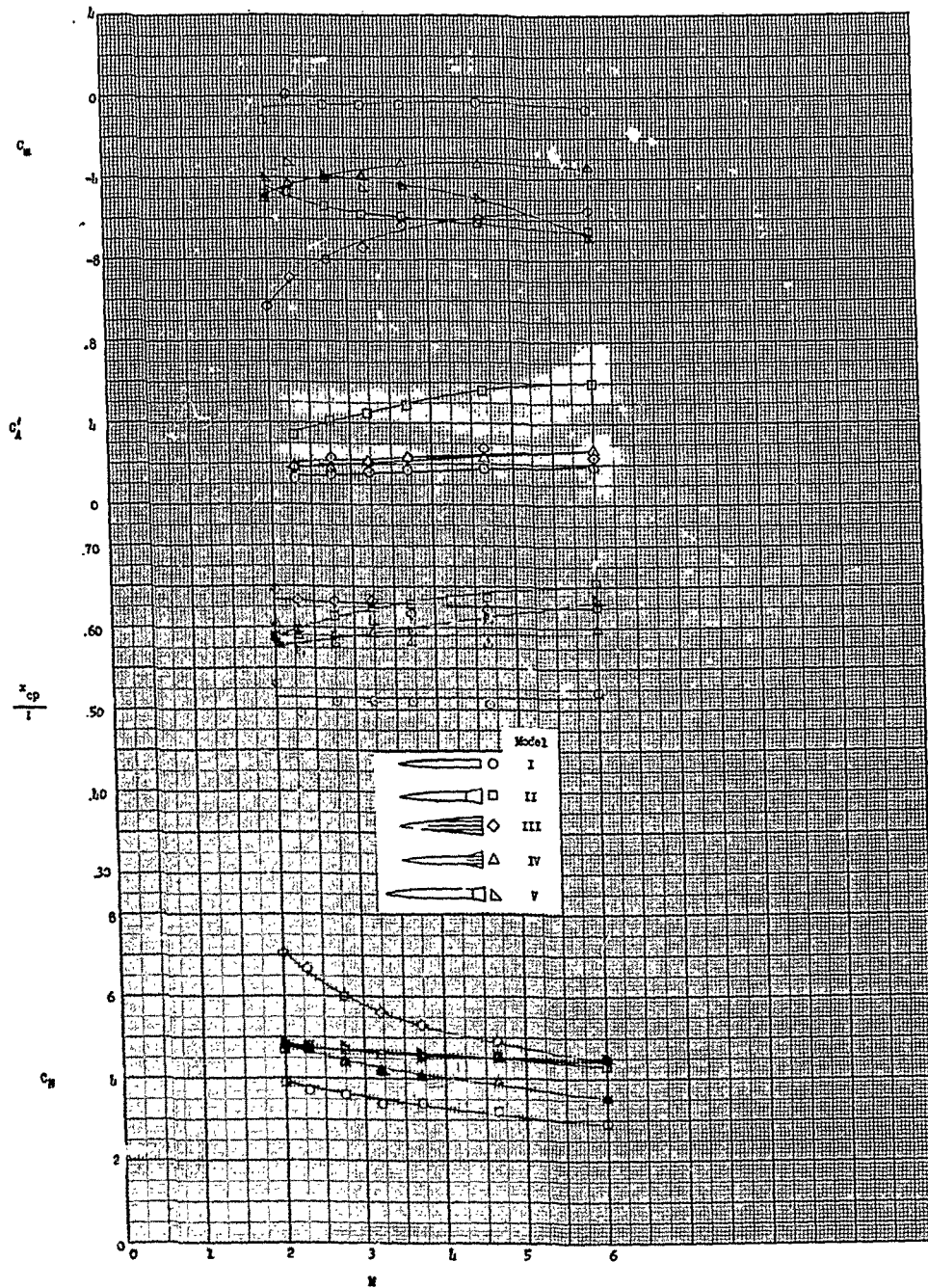
L-934

(b) α = 16°.

Figure 14.- Continued.

CONFIDENTIAL

(c) $\alpha = 24°$.

Figure 14.- Concluded.

CONFIDENTIAL